

Electronic Supplementary Material

for

Polarized light pollution of fixed-tilt photovoltaic solar panels measured by drone-polarimetry and its visual-ecological importance

Péter Takács^{1,2}, Dénes Száz¹, Balázs Bernáth^{1,2}, István Pomozi², Gábor Horváth^{1,*}

1: Environmental Optics Laboratory, Department of Biological Physics, ELTE Eötvös Loránd University, H-1117 Budapest, Pázmány sétány 1, Hungary

2: Drem Innovation and Consulting Ltd., H-1033 Budapest, Szentendrei út 95., Hungary,

peter.takacs@drem.hu (orcid: 0000-0002-5668-0901)

(orcid: 0000-0002-9087-0928)

(orcid: 0000-0003-1712-3288)

(orcid: 0009-0004-6474-2764)

**Corresponding author, e-mail address: gh@arago.elte.hu (orcid: 0000-0002-9008-2411)*

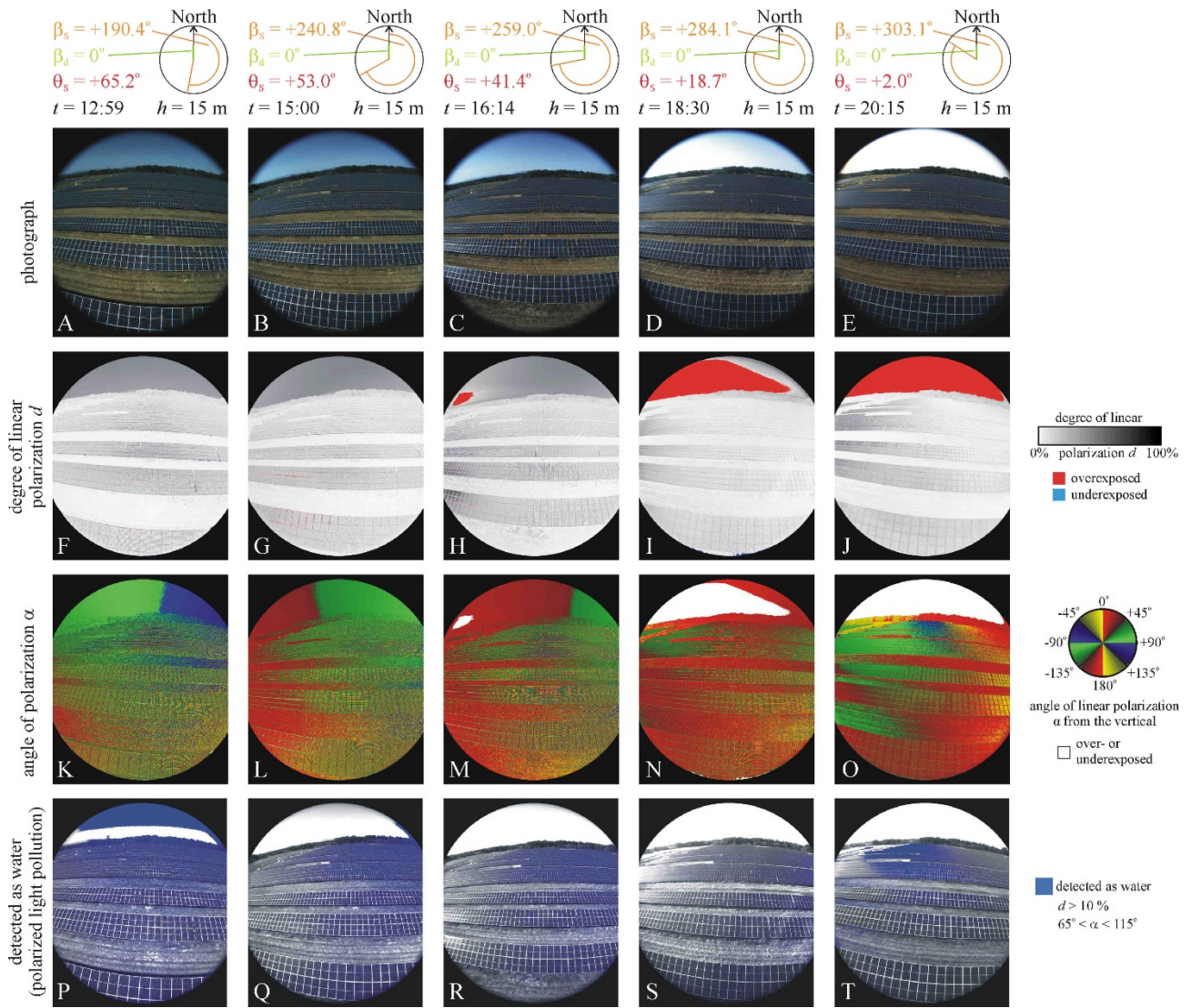
This file contains the following: Supplementary Tables S1, S2
Supplementary Figures S1, S2, S3, S4, S5, S6

Supplementary Table S1: Polarized light pollution plp (%) of solar panels versus time t (local summer time = UTC + 2 h) from sunrise to sunset on the sunny day (30 June 2022) when the drone-polarimeter's azimuth was perpendicular (pointing toward North) and parallel (pointing toward East) to the solar panel rows being parallel to East-West.

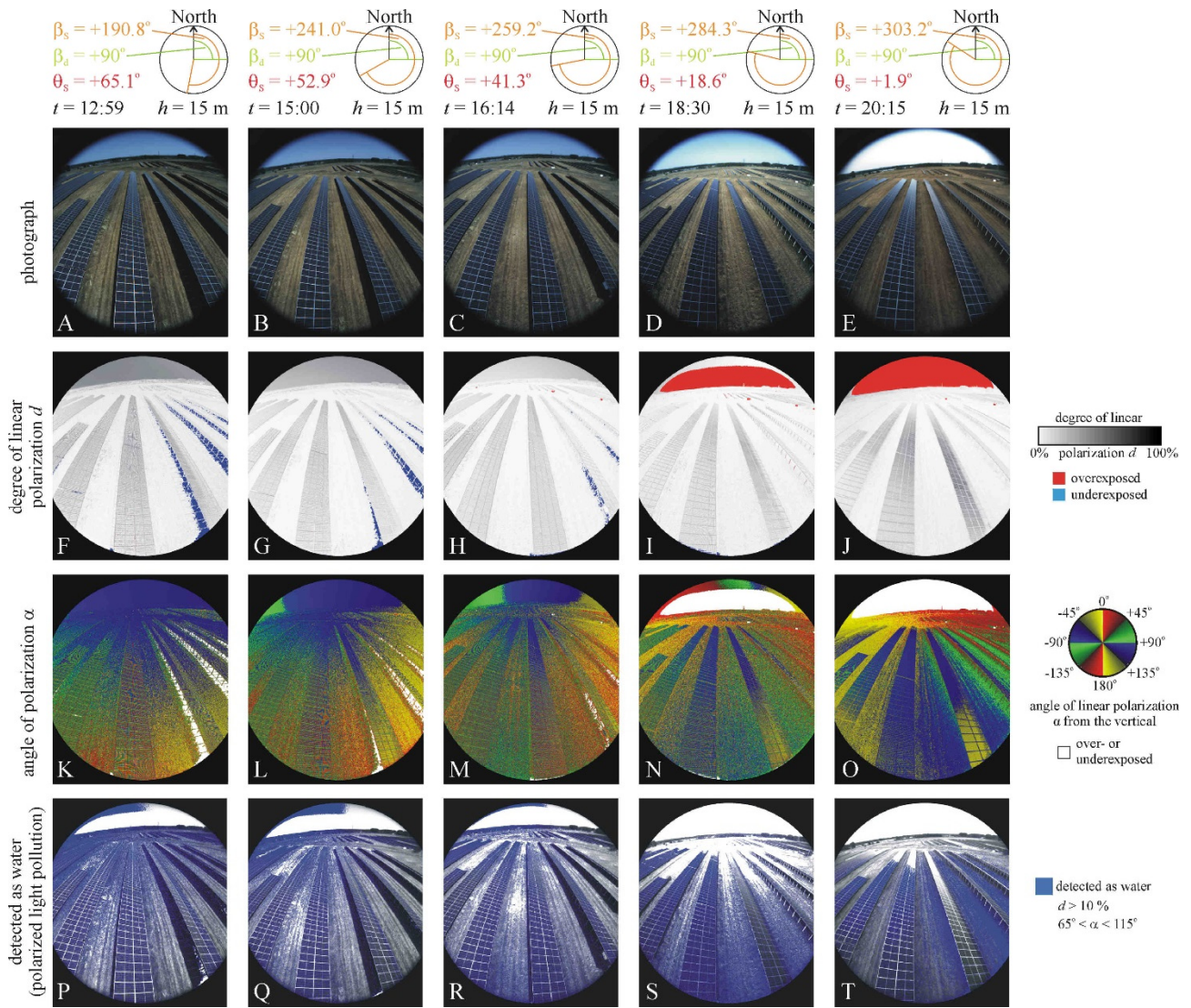
Figure (ID number)	situation	time (UTC + 2 h)	plp ($d > 10\%$, $65^\circ < \alpha < 115^\circ$)
Fig. 2A,E,I,M (438)	sunny 1, perpendicular, North	5:01	16.68 %
Fig. 2B,F,J,N (247)	sunny 2, perpendicular, North	7:01	9.53 %
Fig. 2C,G,K,O (190)	sunny 3, perpendicular, North	8:58	20.63 %
Fig. 2D,H,L,P (181)	sunny 4, perpendicular, North	10:58	26.98 %
Fig. S1A,F,K,P (163)	sunny 5, perpendicular, North	12:59	28.94 %
Fig. S1B,G,L,Q (166)	sunny 6, perpendicular, North	15:00	21.99 %
Fig. S1C,H,M,R (187)	sunny 7, perpendicular, North	16:14	20.36 %
Fig. S1D,I,N,S (180)	sunny 8, perpendicular, North	18:30	7.50 %
Fig. S1E,J,O,T (166)	sunny 9, perpendicular, North	20:15	14.29 %
Fig. 3A,E,I,M (468)	sunny 1, parallel, East	5:01	52.39 %
Fig. 3B,F,J,N (267)	sunny 2, parallel, East	7:01	58.46 %
Fig. 3C,G,K,O (214)	sunny 3, parallel, East	8:58	57.07 %
Fig. 3D,H,L,P (196)	sunny 4, parallel, East	10:58	46.20 %
Fig. S2A,F,K,P (184)	sunny 5, parallel, East	12:59	31.67 %
Fig. S2B,G,L,Q (184)	sunny 6, parallel, East	15:00	29.96 %
Fig. S2C,H,M,R (208)	sunny 7, parallel, East	16:14	29.88 %
Fig. S2D,I,N,S (199)	sunny 8, parallel, East	18:30	35.01 %
Fig. S2E,J,O,T (187)	sunny 9, parallel, East	20:15	25.98 %

Supplementary Table S2: Polarized light pollution plp (%) of solar panels versus time t (local summer time = UTC + 2 h) from sunrise to sunset on the overcast day (24 August 2022) when the drone-polarimeter's azimuth was perpendicular (pointing toward North) and parallel (pointing toward East) to the solar panel rows being parallel to East-West.

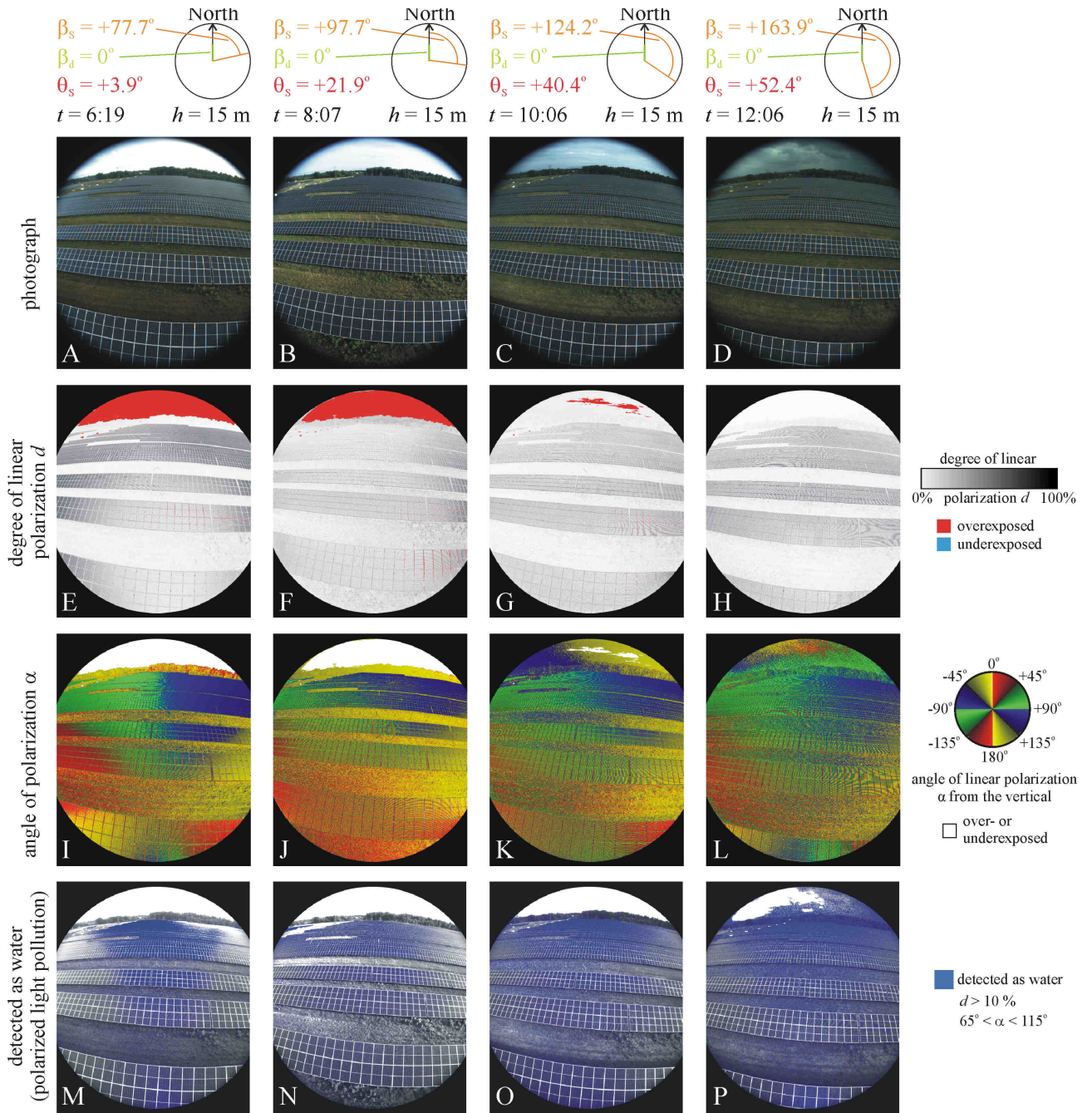
Figure (ID number)	situation	time (UTC + 2 h)	plp ($d > 10$ %, $65^\circ < \alpha < 115^\circ$)
Fig. S3A,E,I,M (238)	overcast 1, perpendicular, North	6:19	27.41 %
Fig. S3B,F,J,N (208)	overcast 2, perpendicular, North	8:07	17.23 %
Fig. S3C,G,K,O (139)	overcast 3, perpendicular, North	10:06	28.38 %
Fig. S3D,H,L,P (079)	overcast 4, perpendicular, North	12:06	34.57 %
Fig. S4A,E,I,M (164)	overcast 5, perpendicular, North	14:11	28.17 %
Fig. S4B,F,J,N (148)	overcast 6, perpendicular, North	16:05	31.69 %
Fig. S4C,G,K,O (103)	overcast 7, perpendicular, North	18:05	26.22 %
Fig. S4D,H,L,P (118)	overcast 8, perpendicular, North	19:34	12.13 %
Fig. S5A,E,I,M (263)	overcast 1, parallel, East	6:20	36.82 %
Fig. S5B,F,J,N (241)	overcast 2, parallel, East	8:08	49.15 %
Fig. S5C,G,K,O (172)	overcast 3, parallel, East	10:07	38.20 %
Fig. S5D,H,L,P (103)	overcast 4, parallel, East	12:05	32.40 %
Fig. S6A,E,I,M (191)	overcast 5, parallel, East	14:12	29.56 %
Fig. S6B,F,J,N (178)	overcast 6, parallel, East	16:06	39.29 %
Fig. S6C,G,K,O (130)	overcast 7, parallel, East	18:06	35.19 %
Fig. S6D,H,L,P (145)	overcast 8, parallel, East	19:35	48.20 %



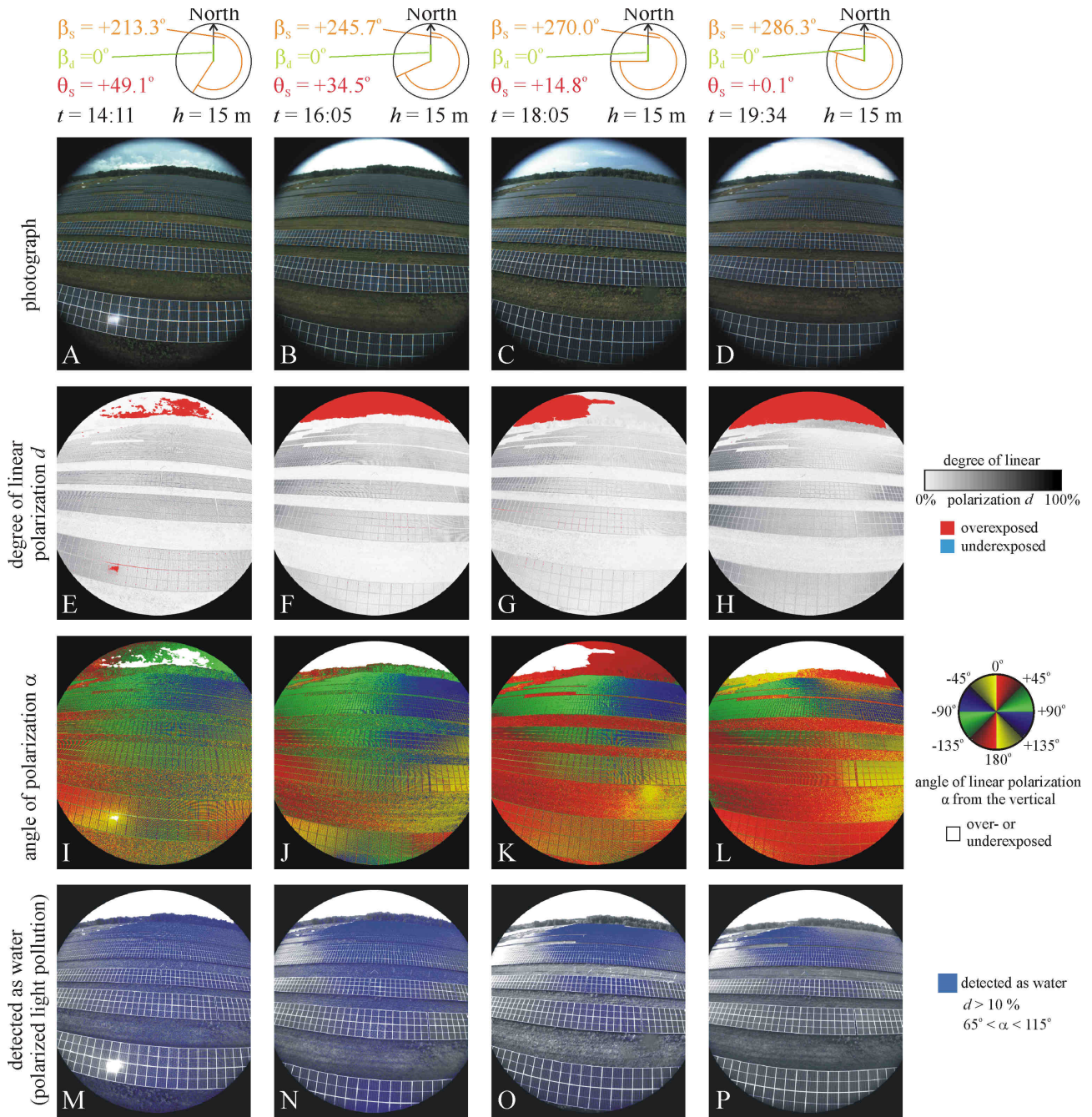
Supplementary Figure S1: Continuation of Fig. 2. From noon to sunset: (A, F, K, P) $t = 12:59$, $h = 15$ m, $\beta_s = +190.41^\circ$, $\theta_s = +65.16^\circ$, $\beta_d = 0^\circ$. (B, G, L, Q) $t = 15:00$, $h = 15$ m, $\beta_s = +240.84^\circ$, $\theta_s = +52.98^\circ$, $\beta_d = 0^\circ$. (C, H, M, R) $t = 16:14$, $h = 15$ m, $\beta_s = +259.01^\circ$, $\theta_s = +41.41^\circ$, $\beta_d = 0^\circ$. (D, I, N, S) $t = 18:30$, $h = 15$ m, $\beta_s = +284.14^\circ$, $\theta_s = +18.7^\circ$, $\beta_d = +0^\circ$. (E, J, O, T) $t = 20:15$, $h = 15$ m, $\beta_s = +303.09^\circ$, $\theta_s = +1.98^\circ$, $\beta_d = +0^\circ$.



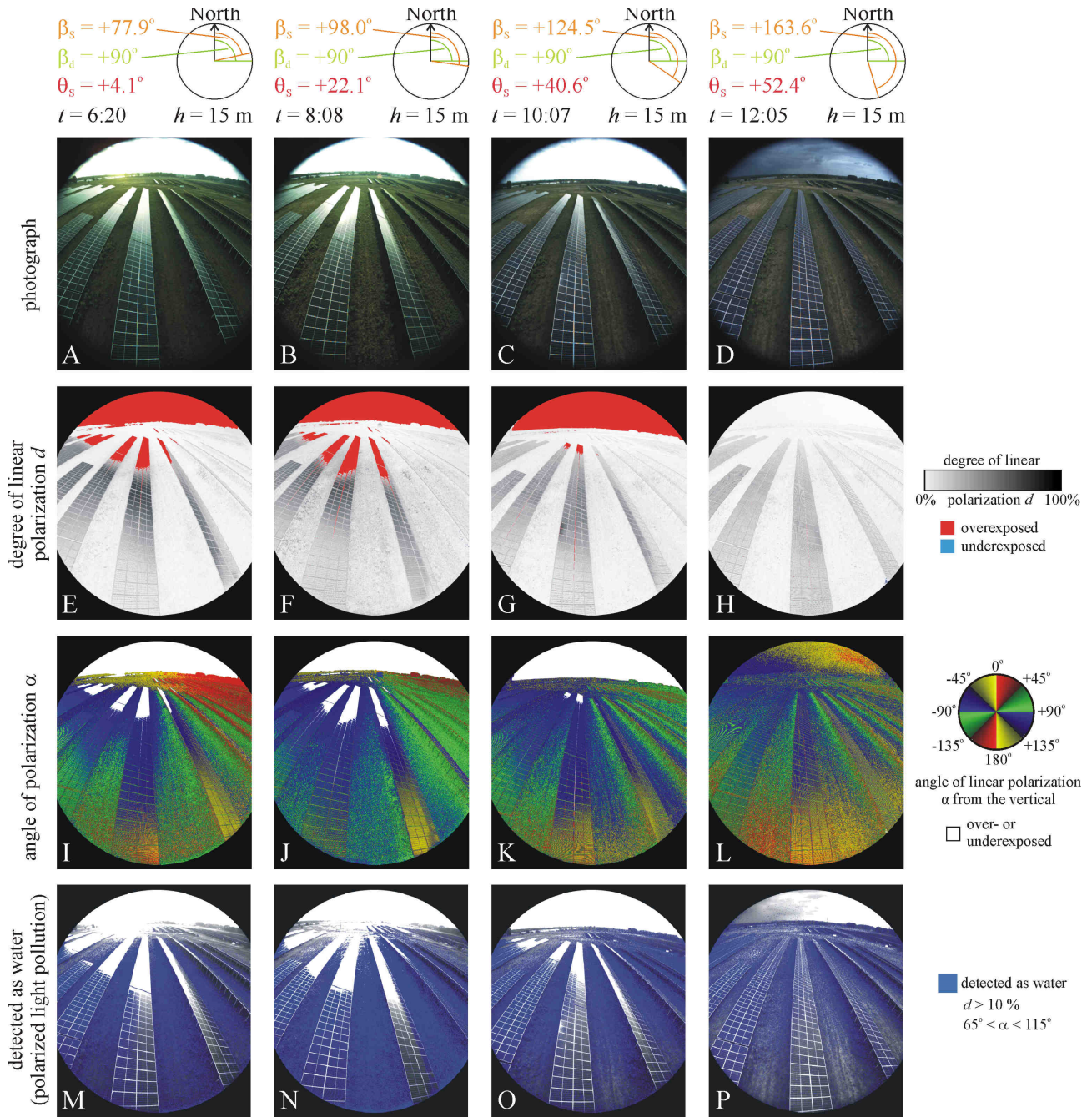
Supplementary Figure S2: Continuation of Fig. 3. From noon to sunset: (A, F, K, P) $t = 12:59$, $h = 15 \text{ m}$, $\beta_s = +190.79^\circ$, $\theta_s = +65.14^\circ$, $\beta_d = +90^\circ$. (B, G, L, Q) $t = 15:00$, $h = 15 \text{ m}$, $\beta_s = +241.01^\circ$, $\theta_s = +52.89^\circ$, $\beta_d = +90^\circ$. (C, H, M, R) $t = 16:14$, $h = 15 \text{ m}$, $\beta_s = +259.16^\circ$, $\theta_s = +41.29^\circ$, $\beta_d = +90^\circ$. (D, I, N, S) $t = 18:30$, $h = 15 \text{ m}$, $\beta_s = +284.25^\circ$, $\theta_s = +18.6^\circ$, $\beta_d = +90^\circ$. (E, J, O, T) $t = 20:15$, $h = 15 \text{ m}$, $\beta_s = +303.22^\circ$, $\theta_s = +1.88^\circ$, $\beta_d = +90^\circ$.



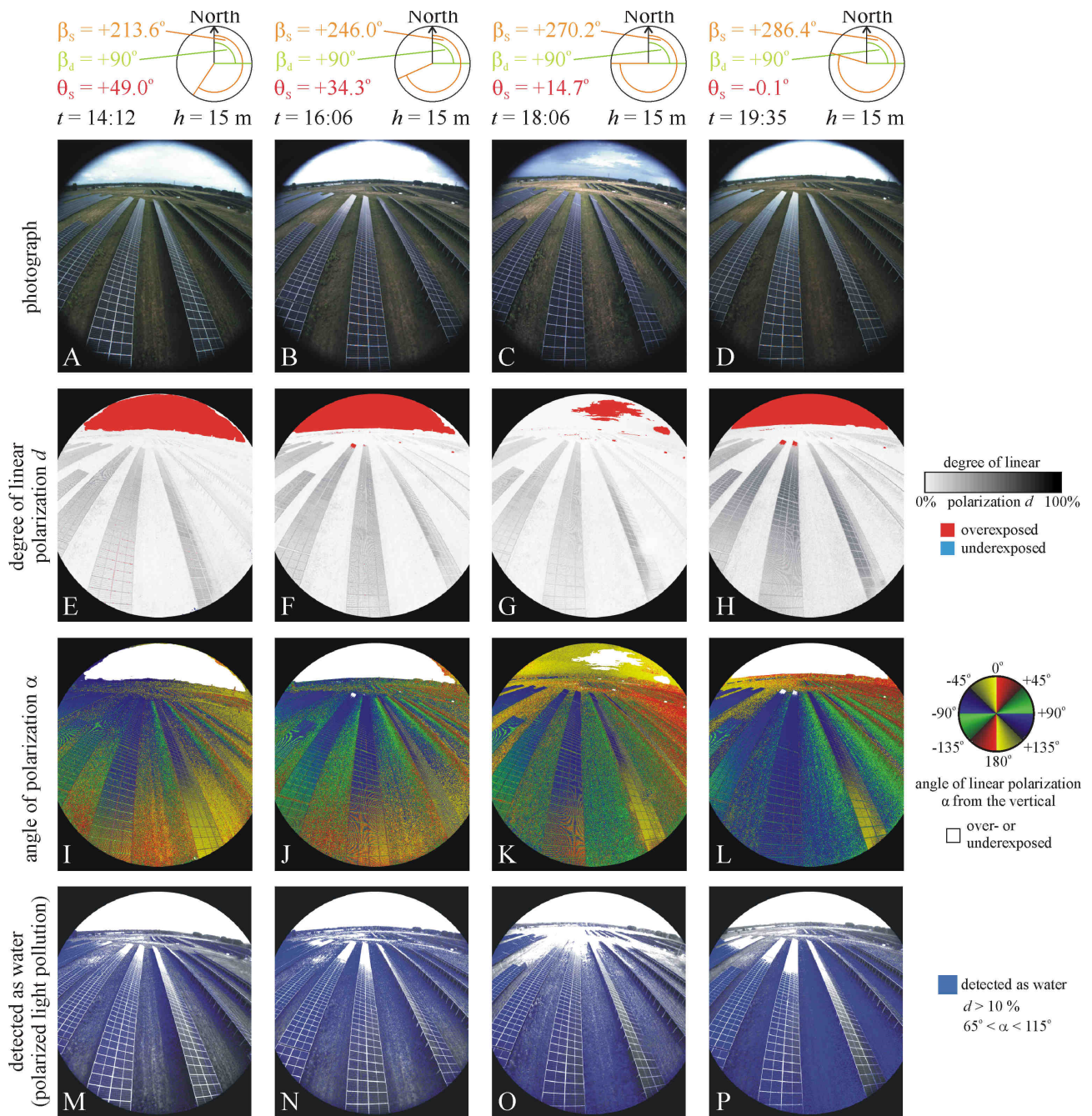
Supplementary Figure S3: As Supplementary Fig. S1 measured on an overcast day (24 August 2022) when the azimuth of the drone's optical axis was perpendicular to the panel rows. From sunrise to noon: (A, E, I, M) $t = 6:19$, $h = 15$ m, $\beta_s = +77.73^\circ$, $\theta_s = +3.88^\circ$, $\beta_d = +0^\circ$. (B, F, J, N) $t = 8:07$, $h = 15$ m, $\beta_s = +97.73^\circ$, $\theta_s = +21.94^\circ$, $\beta_d = +0^\circ$. (C, G, K, O) $t = 10:06$, $h = 15$ m, $\beta_s = +124.17^\circ$, $\theta_s = +40.42^\circ$, $\beta_d = +0^\circ$. (D, H, L, P) $t = 12:06$, $h = 15$ m, $\beta_s = +163.92^\circ$, $\theta_s = +52.39^\circ$, $\beta_d = +0^\circ$.



Supplementary Figure S4: Continuation of Supplementary Fig. S3. From noon to sunset: (A, E, I, M) $t = 14:11$, $h = 15 \text{ m}$, $\beta_s = +213.32^\circ$, $\theta_s = +49.1^\circ$, $\beta_d = 0^\circ$. (B, F, J, N) $t = 16:05$, $h = 15 \text{ m}$, $\beta_s = +245.73^\circ$, $\theta_s = +34.45^\circ$, $\beta_d = 0^\circ$. (C, G, K, O) $t = 18:05$, $h = 15 \text{ m}$, $\beta_s = +270.04^\circ$, $\theta_s = +14.83^\circ$, $\beta_d = 0^\circ$. (D, H, L, P) $t = 19:34$, $h = 15 \text{ m}$, $\beta_s = +286.27^\circ$, $\theta_s = +0.07^\circ$, $\beta_d = 0^\circ$.



Supplementary Figure S5: As Supplementary Fig. S3 when the azimuth of the drone's optical axis was parallel to the panel rows. From sunrise to noon: (A, E, I, M) $t = 6:20$, $h = 15 \text{ m}$, $\beta_s = +77.91^\circ$, $\theta_s = +4.05^\circ$, $\beta_d = +90^\circ$. (B, F, J, N) $t = 8:08$, $h = 15 \text{ m}$, $\beta_s = +97.95^\circ$, $\theta_s = +22.12^\circ$, $\beta_d = +90^\circ$. (C, G, K, O) $t = 10:07$, $h = 15 \text{ m}$, $\beta_s = +124.47^\circ$, $\theta_s = +40.58^\circ$, $\beta_d = +90^\circ$. (D, H, L, P) $t = 12:05$, $h = 15 \text{ m}$, $\beta_s = +163.61^\circ$, $\theta_s = +52.36^\circ$, $\beta_d = +90^\circ$.



Supplementary Figure S6: Continuation of Supplementary Fig. S5. From noon to sunset: (A, E, I, M) $t = 14:12$, $h = 15$ m, $\beta_s = +213.63^\circ$, $\theta_s = +49.01^\circ$, $\beta_d = +90^\circ$. (B, F, J, N) $t = 16:06$, $h = 15$ m, $\beta_s = +245.96^\circ$, $\theta_s = +34.3^\circ$, $\beta_d = +90^\circ$. (C, G, K, O) $t = 18:06$, $h = 15$ m, $\beta_s = +270.21^\circ$, $\theta_s = +14.68^\circ$, $\beta_d = +90^\circ$. (D, H, L, P) $t = 19:35$, $h = 15$ m, $\beta_s = +286.43^\circ$, $\theta_s = -0.07^\circ$, $\beta_d = +90^\circ$.